

Identifying the best iron-peak and α -capture elements for chemical tagging: The impact of the number of lines on measured scatter (Research Note)

V. Adibekyan¹, P. Figueira¹, N. C. Santos^{1,2}, S. G. Sousa¹, J. P. Faria^{1,2}, E. Delgado-Mena¹, M. Oshagh¹, M. Tsantaki¹, A. A. Hakobyan³, J. I. González Hernández^{4,5}, L. Suárez-Andrés^{4,5}, and G. Israelian^{4,5}

¹ Instituto de Astrofísica e Ciências do Espaço, Universidade do Porto, CAUP, Rua das Estrelas, 4150-762 Porto, Portugal

² Departamento de Física e Astronomia, Faculdade de Ciências, Universidade do Porto, Rua do Campo Alegre, 4169-007 Porto, Portugal

³ Byurakan Astrophysical Observatory, 0213 Byurakan, Aragatsotn province, Armenia

⁴ Instituto de Astrofísica de Canarias, 38200 La Laguna, Tenerife, Spain

⁵ Departamento de Astrofísica, Universidad de La Laguna, 38206 La Laguna, Tenerife, Spain

Received date / Accepted date

Abstract

Aims. The main goal of this work is to explore which elements carry the most information about the birth origin of stars and as such that are best suited for chemical tagging.

Methods. We explored different techniques to minimize the effect of outlier value lines in the abundances by using Ni abundances derived for 1111 FGK type stars. We evaluated how the limited number of spectral lines can affect the final chemical abundance. Then we were able to make an efficient even footing comparison of the [X/Fe] scatter between the elements that have different number of observable spectral lines in the studied spectra.

Results. We found that the most efficient way of calculating the average abundance of elements when several spectral lines are available is to use a weighted mean (WM) where as a weight we considered the distance from the median abundance. This method can be effectively used without removing suspected outlier lines. We showed that when the same number of lines is used to determine chemical abundances, the [X/Fe] star-to-star scatter for iron group and α -capture elements is almost the same. On top of this, but at a lower level the largest scatter was observed for Al and the smallest for Cr and Ni.

Conclusions. We recommend caution when comparing [X/Fe] scatters among elements that have a different number of spectral lines available. A meaningful comparison is necessary to identify elements that show the largest intrinsic scatter and can be thus used for chemical tagging.

Key words. stars: abundances – stars: general – stars: fundamental parameters

1. Introduction

Studies of large samples of stars are very important for understanding the Galactic and stellar chemical evolution. Understanding the effects of these two mechanisms is, in turn, crucial for the studies of chemical properties of individual stars. A representative example is the so-called T_c -trend: a trend of chemical abundance with the condensation temperature of the elements, whose real nature is still under debate (e.g. Meléndez et al. 2009; Ramírez et al. 2009; González Hernández et al. 2010, 2013; Schuler et al. 2011; Adibekyan et al. 2014; Önehag et al. 2014; Maldonado et al. 2015; Nissen 2015).

Precise and detailed chemical composition studies of large samples of stars are also of great importance for different venues of Galactic astronomy. One of these venues goes towards a so-called chemical tagging technique: identifying stars with identical chemical properties. This technique was introduced by Freeman & Bland-Hawthorn (2002), and then explored and developed by many other authors (e.g. De Silva et al. 2006; Tabernero et al. 2012, 2014; Mitschang et al. 2013, 2014; Blanco-Cuaresma et al. 2015). Chemical tagging is a very pow-

erful tool to identify stellar groups and clusters (e.g. Tabernero et al. 2014; De Silva et al. 2013; Spina et al. 2014a,b; Quillen et al. 2015) and even to identify solar siblings (e.g. Batista et al. 2014; Ramírez et al. 2014; Liu et al. 2015).

In all likelihood, not all elements are equally useful for chemical tagging. A way of selecting the elements that can be used to tag stars is to look at the star-to-star [X/Fe] abundance ratio scatter at solar metallicities, where the Galactic chemical evolution does not have a very strong effect. Elements that show largest star-to-star scatter are the more informative, being of physical origin.

The works of De Silva et al. (2006, 2007, 2009) on open clusters and those of Ramírez et al. (2009) and González Hernández et al. (2010) for solar-twins/analogs clearly show that most of the elements show very small star-to-star [X/Fe] scatter. These authors performed a fully differential chemical abundance analysis in a line-by-line basis with respect to a solar spectrum reference, as well as to a star which is expected to belong to a given open cluster or kinematical group. In particular, in the recent work of Ramírez et al. (2014), a higher weight/priority to Na, Al, V, Y, and Ba were given for chemical tagging. However, in

all the mentioned studies when the star-to-star $[X/Fe]$ scatters were compared for different elements, an important parameter was not taken into account: the number of spectral lines used to derive abundances for each element.

In this work, using a large and high-quality data of solar-type stars, we study the dependence of $[X/Fe]$ scatter on the number of spectral lines. This allows us to make a comparison on the same ground of the $[X/Fe]$ scatter for different elements by using the same number of lines. Our sample comes from Adibekyan et al. (2012) and consists of 1111 FGK-type dwarfs observed with the high-resolution HARPS spectrograph. The stellar parameters and abundances of the stars were derived from the high signal-to-noise ratio (SNR) spectra with a median SNR of 235 (only 15% of the spectra have SNR < 100).

We organize our paper as follows. In Appendix A, we quantify the precision in the abundance value as a function of number of spectral lines and summarize the results in Sect. 2. The discussion on the $[X/Fe]$ star-to-star abundance scatter and conclusions are presented in Sects 3 and 4.

2. Reducing the impact of outlier lines

The data used in this work was taken from Adibekyan et al. (2012), which provides chemical abundances for 12 iron-peak and α -capture elements (15 ionized or neutral species). In the present paper we did not use the final (average) abundances of different elements, but instead we used the abundances derived from individual lines of each element. As stated previously, this is because we aim at studying the dependence of precision in abundances on the number of lines.

A standard, and widely used technique to calculate chemical abundances derived from several spectral lines is to apply an outlier removal criteria and then calculate the arithmetic mean (AM) of the abundances from the remaining lines. However, the detection of outliers is not an easy task. There are several outlier removal methods discussed in the literature (e.g. σ -clipping (e.g. Shiffler 1988), modified Z-score (Iglewicz & Hoaglin 1993), Tukey’s (boxplot) method (Tukey 1977), and median-rule (Carling 1998)), however most of them are model dependent while depending on the applied threshold for which there is no clear prescription or theoretical ground. It is appropriate to note, that outlier removal is not the only method used to characterize an underlying distribution in a dataset. An example is the weighted least-squares regression to minimize the effects of outlier data (Rousseeuw & Leroy 1987).

In Appendix A, we present an comprehensive discussion about different outlier methods and a new WM method where as weight we use (inverse) distance from the median value as measured in units of standard deviations (SD). We made several tests to evaluate the impact of outliers on the chemical abundances (using Ni for our tests), and the dependence of the precision of the abundances on the number of lines.

Our tests showed that when the number of lines is large, different outlier removal techniques and criteria provide similar final abundances. However, the line-to-line dispersion, which is usually used to estimate the error on abundances, strongly depends on the criteria and can be artificially (unrealistically) reduced depending on the outlier removal method and threshold. We conclude and recommend to use the WM (instead of any outlier removal technique) when several lines are available at hand.

We found that even for solar-type stars for which high-quality data is available, significant deviations in abundances from the real value are possible when the number of lines is small.

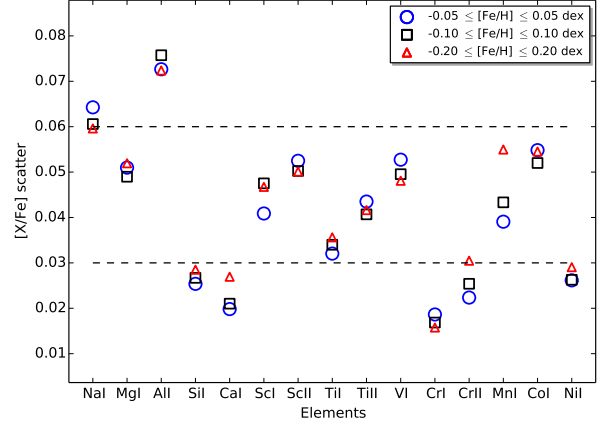


Figure 1. $[X/Fe]$ star-to-star scatter for solar-analogs with solar-metallicity. The dashed lines, which represent $[X/Fe] = 0.03$ and 0.06 dex, are just to make the comparison of the $[X/Fe]$ scatters between the elements visually easier.

We refer the interested reader to Appendix A for the details of the tests and discussion.

3. $[X/Fe]$ star-to-star scatter

Recently, several works on solar analogs (e.g. Ramírez et al. 2009; González Hernández et al. 2010, 2013), showed that the $[X/Fe]$ versus $[Fe/H]$ trends show very small star-to-star scatter at the solar metallicities for most of the elements. In Fig. 1, we plot $[X/Fe]$ scatter (*rms*) for dwarf stars ($\log g \geq 4$ dex) that have effective temperatures within 300 K of that of the Sun ($T_{eff} \leq 5777 \pm 300$ K) and have metallicities in the range of $[Fe/H] = 0.0 \pm 0.05$, $[Fe/H] = 0.0 \pm 0.10$, and $[Fe/H] = 0.0 \pm 0.20$ dex, respectively. The abundances of all the elements were derived using all the available lines by applying the WM technique. We selected only stars with solar metallicities to minimize the effect of Galactic chemical evolution and the thin/thick disk dichotomy (however see the discussion in Adibekyan et al. 2011, 2013, about thin/thick disk separation at solar and super-solar metallicities). The constrain on T_{eff} serves to select the stars with the highest precision of the stellar parameters and chemical abundances (Sousa et al. 2008; Adibekyan et al. 2012; Tsantaki et al. 2013). We note that the sample size is large enough to minimize the errors related to the sampling of the population. For example, if the scatter (standard deviation) is of about 0.05 dex (which is the case for most of the elements), the 95% confidence interval of this value would be from 0.045 to 0.056 for the sample size of 152 (the number of stars in the metallicity range of 0.0 ± 0.10 dex)¹.

Fig. 1 shows that the highest scatter is observed for Na and Al, and the $[X/Fe]$ scatter for Si, Ca, Cr, and Ni is the lowest. The number of available lines that were used to derive abundances of Na and Al is the lowest: only two lines, while elements showing the smallest scatter usually have more than 10 lines. From the figure, it is apparent that the scatter does not change much when different metallicity intervals are used. The only exception is Mn where scatter increases with the width of the metallic-

¹ The confidence interval of SD can be calculated as presented in Sheskin (2007).

ity interval. We note, that for the derivation of Mn abundances we did not consider hyperfine structure (hfs), which is important for odd-Z elements and, if not considered might overestimate the Mn abundances deduced from a given EW. This can be one of the reasons for the observed increase of $[\text{Mn}/\text{Fe}]$ scatter with metallicity. Another reason for the observed high scatter at larger range of $[\text{Fe}/\text{H}]$ could be the strong Galactic evolution trend in the $[\text{Mn}/\text{Fe}] - [\text{Fe}/\text{H}]$ plane at solar metallicities (e.g. Adibekyan et al. 2012; Battistini & Bensby 2015). We note, that the trend is strong even if the hfs effect, but not a non-LTE effect is taken into account (e.g. Battistini & Bensby 2015).

To evaluate the impact of the number of lines (e.g. precision) on the $[\text{X}/\text{Fe}]$ scatter we did a test similar to that presented in the previous section (see Appendix A for the details). For each element, we randomly drew N number of lines (where N is from one to the maximum number of lines) and calculated the $[\text{X}/\text{Fe}]$ scatter for solar analogs in the metallicity range of 0.0 ± 0.10 dex. If the number of possible combinations of the lines is less than 1000 we considered all of them, else we limited ourselves to fixed number of 1000 random (but different i.e., without replacement) combinations.

In Fig. B.1, we plot the dependence of $[\text{X}/\text{Fe}]$ star-to-star scatter as a function of the number of lines that were used for $[\text{X}/\text{H}]$ abundance derivations. The plot clearly shows that the average scatter decreases with the number of lines. The plot also shows that the WM always gives smaller scatter than the AM (of course, when the number of lines is larger than two). This fact can be considered as an independent confirmation of the better “precision” of the abundances calculated using WM technique.

It is also very interesting to note that some individual lines can introduce a very large scatter while others provide very small one. The results of this test can be used to rank the spectral lines according to the $[\text{X}/\text{Fe}]$ scatter they provide. This can be used as a “new” method to eliminate outliers and select the best possible lines. For example, there is one Ca line ($\lambda 5261.71$) that clearly shows a very large scatter (0.16 dex) compared to the rest of 12 lines (on average ≈ 0.06 dex). It is interesting and important to note, that the average difference of the $[\text{Ca}/\text{H}]$ abundance derived by using this line from the mean abundance is very small, but again with a large dispersion $\langle \Delta[\text{Ca}/\text{H}] \rangle = 0.05 \pm 0.15$ dex, which means that the line does not show systematically higher or lower abundance when compared to that derived with the remaining lines. If all the 1111 stars are considered, then this difference becomes smaller, and negative $\langle \Delta[\text{Ca}/\text{H}] \rangle = -0.02 \pm 0.15$ dex. Our analysis of the $[\text{Ca}/\text{Fe}]$ versus T_{eff} for this line shows a very weak trend (0.05 dex/1000K) and particularly large scatter at low temperatures. However we found that the deviation of the Ca abundance of this line from the mean Ca abundance depends on the EW. The average EW of this line is 104 ± 23 and 116 ± 45 mÅ for the solar analogs and for all the stars, respectively. When the EW is greater than 100 mÅ, the deviation increases significantly.

Similar to the discussed Ca line, we found some lines for the other elements that show distinguishably large dispersion. We provide the ranked list of all the lines ordered by the scatter size².

Using the $[\text{X}/\text{Fe}]$ scatter for all the elements and for different number of lines, we compared the $[\text{X}/\text{Fe}]$ star-to-star scatter for different elements using the same number of lines in Fig. 2. We plot the scatter derived using 2, 6, 13, and 20 lines because these numbers are those that better match the number of lines available: maximizing the number of lines and elements in the

panels. For example, all the elements have at least two lines, and there is only one element that has a number of lines between 6 and 13.

The top-left panel of Fig. 2 shows that when only two lines are used for all the elements to calculate $[\text{X}/\text{Fe}]$, almost all the elements show a similar scatter of about 0.06 dex. Aluminum shows the largest, and Cr and Ni show the smallest scatters. However, one can also see that depending on the combinations of lines the $[\text{X}/\text{Fe}]$ scatter can be different for the same element (the error bar in the plot). The other three panels, that provide information which is more statistically significant since it is based on larger number of lines, show that from elements that have at least six lines, Ti, V, ScII, and Co show the largest scatter. Again, Cr and Ni show the smallest scatter. We note that although the obtained differences in $[\text{X}/\text{Fe}]$ scatter between elements are not large, they are based on a large sample and thus can be considered statistically significant.

The decrease of the $[\text{X}/\text{Fe}]$ scatter with the number of lines means that a fraction of the observed scatter does not have astrophysical origin. Table 3 of Adibekyan et al. (2012) provides the average error of the $[\text{X}/\text{Fe}]$ ratios for the same sample of stars. The table shows that the average error varies from 0.01 to 0.03 dex. For the elements that have at least 13 lines (SiI, CaI, TiI, CrI, and NiI) the average error on $[\text{X}/\text{Fe}]$ is 0.01 dex.

Our results show the importance of the initial selection of the lines, especially when the number of lines is small. By carefully selecting lines for individual stars with a given set of stellar parameters and a given quality of the spectra, one can derive precise chemical abundances even when the number of lines is small and have small $[\text{X}/\text{Fe}]$ scatter, as already demonstrated by e.g., Ramírez et al. (2009) and González Hernández et al. (2010) for solar analog stars. However, when dealing with large number of stars with different combinations of stellar parameters and quality of the spectra, it is not realistic to control abundances of each individual line in each individual star.

4. Summary and conclusion

In this paper, we used a large sample of FGK stars (Adibekyan et al. 2012) to study the dependence of precision of chemical abundances on the number of lines and how it affects the $[\text{X}/\text{Fe}]$ star-to-star scatter at solar metallicities. We explored different techniques to calculate the mean abundance and minimize the effect of possible outliers when several spectral lines are available for an element.

From our tests we conclude and recommend to use the WM (instead of any outlier removal technique) when several lines are available at hand. As a weight, the distance from the median abundance can be effectively used, as demonstrated.

Selecting only solar-analogs with metallicities similar to that of the Sun by 0.10 dex, we showed that $[\text{X}/\text{Fe}]$ scatter strongly depends on the number of lines suggesting that one should be cautious when comparing star-to-star abundance dispersion of elements which abundances were derived using different number of lines. The decrease of scatter with the number of lines suggests that some fraction of the observed scatter has non-astrophysical nature. A large number of lines is needed to reduce the precision induced scatter.

The comparison of the $[\text{X}/\text{Fe}]$ scatter for different elements using the same number of lines show that most elements show a very similar dispersion. The largest scatter among the elements studied in this work was found for Na, Al, Ti, V, ScII, and Co, while Cr and Ni show the smallest scatter. The similarity and

² The table is available at the CDS.

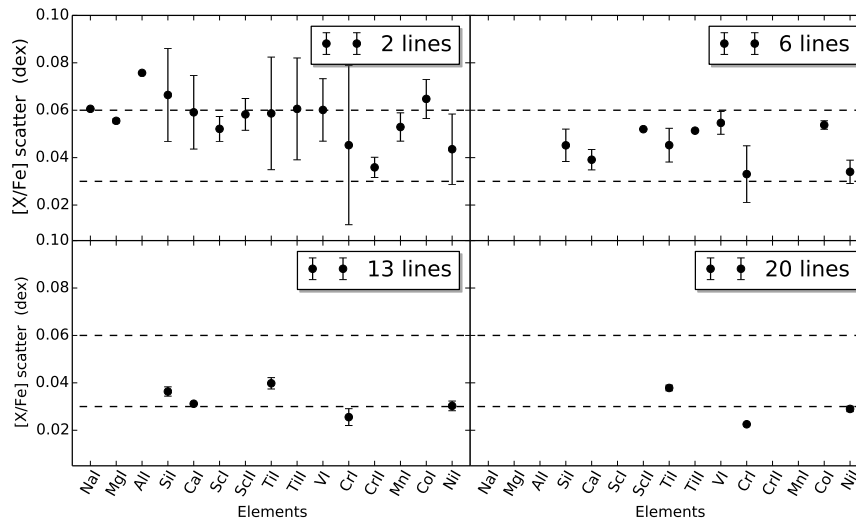


Figure 2. $[X/Fe]$ star-to-star scatter for solar-analogs with solar-metallicity. The $[X/Fe]$ scatter is derived by using 2, 6, 13 and 20 lines. The error bars show the standard deviation of the scatter calculated using different combinations of lines. The dashed lines, which represent $[X/Fe] = 0.03$ and 0.06 dex, are just to make the comparison of the $[X/Fe]$ scatters between the elements visually easier.

differences in $[X/Fe]$ scatter between the elements have different/similar nucleosynthesis production sites (see e.g. Nomoto et al. 2013).

Our group is currently working on the derivation of abundances of volatile (C and N) and r- and s-process elements (Suárez-Andrés et al, in prep; Delgado-Mena et al, in prep). When the data is ready a similar analysis will be done for these elements to select the elements that are the most informative for chemical tagging.

Acknowledgements. This work was supported by Fundação para a Ciência e a Tecnologia (FCT) through the research grant UID/FIS/04434/2013. P.F., N.C.S., and S.G.S. also acknowledge the support from FCT through Investigador FCT contracts of reference IF/01037/2013, IF/00169/2012, and IF/00028/2014, respectively, and POPH/FSE (EC) by FEDER funding through the program “Programa Operacional de Factores de Competitividade - COMPETE”. PF further acknowledges support from Fundação para a Ciência e a Tecnologia (FCT) in the form of an exploratory project of reference IF/01037/2013CP1191/CT0001. V.A. and E.D.M acknowledge the support from the Fundação para a Ciência e Tecnologia, FCT (Portugal) in the form of the grants SFRH/BPD/70574/2010 and SFRH/BPD/76606/2011, respectively. JPF acknowledges the support from FCT through the grant reference SFRH/BD/93848/2013. MO acknowledges support by Centro de Astrofísica da Universidade do Porto through grant with reference of CAUP-15/2014-BDP. JIGH acknowledges financial support from the Spanish Ministry of Economy and Competitiveness (MINECO) under the 2011 Severo Ochoa Program MINECO SEV-2011-0187. This work results within the collaboration of the COST Action TD 1308.

References

Acuna, E. & Rodriguez, C. 2004, *Classification, Clustering and Data Mining Applications*, 639
 Adibekyan, V. Z., Benamati, L., Santos, N. C., et al. 2015, *MNRAS*, 450, 1900
 Adibekyan, V. Z., Figueira, P., Santos, N. C., et al. 2013, *A&A*, 554, A44
 Adibekyan, V. Z., González Hernández, J. I., Delgado Mena, E., et al. 2014, *A&A*, 564, L15
 Adibekyan, V. Z., Santos, N. C., Sousa, S. G., & Israelian, G. 2011, *A&A*, 535, L11
 Adibekyan, V. Z., Sousa, S. G., Santos, N. C., et al. 2012, *A&A*, 545, A32
 Anders, E. & Grevesse, N. 1989, *Geochim. Cosmochim. Acta*, 53, 197
 Batista, S. F. A., Adibekyan, V. Z., Sousa, S. G., et al. 2014, *A&A*, 564, A43
 Battistini, C. & Bensby, T. 2015, *A&A*, 577, A9
 Bertran de Lis, S., Delgado Mena, E., Adibekyan, V. Z., Santos, N. C., & Sousa, S. G. 2015, *A&A*, 576, A89

Blanco-Cuaresma, S., Soubiran, C., Heiter, U., et al. 2015, *A&A*, 577, A47
 Carling, K. 1998, *Resistant outlier rules and the non-Gaussian case*, Working Paper Series 2001:7, IFAU - Institute for Evaluation of Labour Market and Education Policy
 De Silva, G. M., D’Orazi, V., Melo, C., et al. 2013, *MNRAS*, 431, 1005
 De Silva, G. M., Freeman, K. C., Asplund, M., et al. 2007, *AJ*, 133, 1161
 De Silva, G. M., Freeman, K. C., & Bland-Hawthorn, J. 2009, *PASA*, 26, 11
 De Silva, G. M., Sneden, C., Paulson, D. B., et al. 2006, *AJ*, 131, 455
 Freeman, K. & Bland-Hawthorn, J. 2002, *ARA&A*, 40, 487
 González Hernández, J. I., Delgado-Mena, E., Sousa, S. G., et al. 2013, *A&A*, 552, A6
 González Hernández, J. I., Israelian, G., Santos, N. C., et al. 2010, *ApJ*, 720, 1592
 Hodge, V. & Austin, J. 2004, *Artificial Intelligence Review*, 22, 85, copyright 2004 Kluwer Academic Publishers.
 Iglewicz, B. & Hoaglin, D. 1993, *How to Detect and Handle Outliers*, ASQC basic references in quality control (ASQC Quality Press)
 Liu, C., Ruchti, G., Feltzing, S., et al. 2015, *A&A*, 575, A51
 Maldonado, J., Eiroa, C., Villaver, E., Montesinos, B., & Mora, A. 2015, *A&A*, 579, A20
 Meléndez, J., Asplund, M., Gustafsson, B., & Yong, D. 2009, *ApJ*, 704, L66
 Mitschang, A. W., De Silva, G., Sharma, S., & Zucker, D. B. 2013, *MNRAS*, 428, 2321
 Mitschang, A. W., De Silva, G., Zucker, D. B., et al. 2014, *MNRAS*, 438, 2753
 Neves, V., Santos, N. C., Sousa, S. G., Correia, A. C. M., & Israelian, G. 2009, *A&A*, 497, 563
 Nissen, P. E. 2015, *A&A*, 579, A52
 Nomoto, K., Kobayashi, C., & Tominaga, N. 2013, *ARA&A*, 51, 457
 Önehag, A., Gustafsson, B., & Korn, A. 2014, *A&A*, 562, A102
 Quillen, A. C., Anguiano, B., De Silva, G., et al. 2015, *MNRAS*, 450, 2354
 Ramírez, I., Bajkova, A. T., Bobylev, V. V., et al. 2014, *ApJ*, 787, 154
 Ramírez, I., Meléndez, J., & Asplund, M. 2009, *A&A*, 508, L17
 Rousseeuw, P. J. & Leroy, A. M. 1987, *Robust Regression and Outlier Detection* (New York, NY, USA: John Wiley & Sons, Inc.)
 Schuler, S. C., Flateau, D., Cunha, K., et al. 2011, *ApJ*, 732, 55
 Sheskin, D. J. 2007, *Handbook of Parametric and Nonparametric Statistical Procedures*, 4th edn. (Chapman & Hall/CRC)
 Shiffler, R. E. 1988, *The American Statistician*, 42, 79
 Sousa, S. G., Santos, N. C., Mayor, M., et al. 2008, *A&A*, 487, 373
 Spina, L., Randich, S., Palla, F., et al. 2014a, *A&A*, 568, A2
 Spina, L., Randich, S., Palla, F., et al. 2014b, *A&A*, 567, A55
 Tabernero, H. M., Montes, D., & González Hernández, J. I. 2012, *A&A*, 547, A13
 Tabernero, H. M., Montes, D., Gonzalez Hernandez, J. I., & Ammler-von Eiff, M. 2014, *ArXiv e-prints*
 Tsantaki, M., Sousa, S. G., Adibekyan, V. Z., et al. 2013, *A&A*, 555, A150
 Tukey, J. W. 1977, *Exploratory Data Analysis* (Addison-Wesley)

Appendix A: Dependence of abundances on the number of lines: the case of Ni

The data used in this work was taken from Adibekyan et al. (2012), which provides chemical abundances for 12 iron-peak and α -capture elements (15 ionized or neutral species).

The lines used in this work are based on the line-list of Neves et al. (2009). From the VALD³ online database, 180 lines were carefully selected in the solar spectrum to be: not-blended, have Equivalent Widths (EW) above 5 mÅ and below 200 mÅ, be located outside of the wings of very strong lines. Later on, the semi-empirical oscillator strengths for the lines were calculated by calibrating the $\log gf$ values to the solar reference of Anders & Grevesse (1989). Moreover, only “stable” lines which do not show high abundances dispersion (i.e., 1.5 times the *rms*) from the mean abundance for each element were selected. In this later test, 451 stars with wide range of stellar parameters and SNR were used. The selected 180 lines, were re-checked in Adibekyan et al. (2012), where several lines were excluded because of the observed abundance trend $[X/Fe]$ with the effective temperature. For more details about the selection of the lines we refer the reader to Neves et al. (2009) and Adibekyan et al. (2012). Our final line-list consists of 164 lines⁴.

We stress that the main goal in this work is not to re-check the quality of the lines, nor to provide a range of parameter space (stellar parameters and SNR) where each individual line can be safely and reliably used. Since different authors use different set of spectral lines and different atomic data for the lines, for us it is more straightforward and scientifically interesting to discuss methods that can, in principle, effectively work for different line-lists and when applied on large datasets, as it is often the case.

A.1. Comparing methods

In Adibekyan et al. (2012) the final abundance for each star and element was calculated as the arithmetic mean (AM) of the abundances given by all lines detected in a given star and element after a 2- σ -clipping was applied. This is a standard, and widely used technique that allows to avoid the errors caused by bad pixels, bad measurements, cosmic rays, and other unknown localized effects. However, this type of “outlier” removal technique depends on the threshold (2- σ in our case) that is applied for which there is no clear prescription, or theoretical ground, and the choice ends up being very subjective. The choice of threshold should also depend on the sample size. A simple demonstration of this sample size dependence is presented by Shiffler (1988), who showed that the possible maximum Z-score (number of SD a data-point is far from the mean) depends (only) on the sample size and it is computed as $(n-1)/\sqrt{n}$. From this formula we get, that the maximum deviation one can obtain in a sample of 5 points (lines) is 1.79- σ , i.e., no outliers can be identified in the data if 2- σ -clipping is applied. One can alternatively use median and median absolute deviation (MAD), which is expected to be less sensitive to outliers, or apply other outlier removal methods (e.g. Hodge & Austin 2004; Iglewicz & Hoaglin 1993). However, it is very difficult to choose a single method and a criterion that will efficiently work for samples of different size. Moreover, when a certain criterion is applied to remove possible outliers, some valid lines from the real distribution can be

Table A.1. The difference in Ni abundances when WM method and other methods are applied for the derivation of Ni.

Methods	Threshold	ΔNi (dex)
WM – AM	–	-0.0020±0.0096
WM – Median-rule	median±2IQR	0.0001±0.0052
	median±2.5IQR	-0.0002±0.0057
	median±3IQR	-0.0006±0.0062
WM – σ -clipping	median±2SD	0.0003±0.0049
	median±2.5SD	-0.0002±0.0054
	median±3SD	-0.0004±0.0062
WM – MAD _e	median±2.5MAD _e	0.0002±0.0049
	median±3MAD _e	4.5×10 ⁻⁵ ±0.0057
	median±3.5MAD _e	-0.0006±0.0062
WM – MAD _e ^{iter}	median±2.5MAD _e	0.0004±0.0055
	median±3MAD _e	0.0001±0.0052
	median±3.5MAD _e	-0.0002±0.0057

removed as well. Finally, one should also bear in mind that most of the outlier removal methods are model-dependent assuming some distributions for the real and outlier data.

To explore and choose the method that allows to derive the most precise final abundances of the elements, we selected Ni for our analysis because it has the largest linelist (43 lines). By plotting the individual Ni abundances in the full sample of 1111 stars we noticed that many of the stars have Ni lines which show deviation from the average value by more than 3- σ . To understand if these lines are outliers or just extremes of the distribution (a normal distribution is assumed here) we performed some simple calculations. If one assumes a normal distribution, then a 3- σ corresponds to P = 0.003 probability. Since on average we derive Ni abundance from 43 lines, then the probability that we will have at least one “outlier” is of $43 \times 0.003 = 0.129$. This means that among the 1111 stars we expect to have about $0.129 \times 1111 = 143$ stars with one “outlier” line. However, the number of stars which have at least one “outlier” is 626. To estimate the probability of having that many stars with at least one “outlier” we used binomial probability distribution. The probability that more than 200 stars (any number above 200) can have an “outlier” is already 8×10^{-7} . This means that, under our assumption of Gaussian distribution of the abundances derived from different lines, some of the lines which show large dispersion ($> 3\sigma$) can be real outliers of different origin and are not just coming from the wings of the Gaussian distribution. We note, that the results of this test do not depend on the applied threshold (3- σ in this case).

Fortunately, if the linelist is large, the possible outliers do not affect much the final (mean) abundance. We first tested three different outlier removal methods, namely σ -clipping (e.g. Shiffler 1988), modified Z-score (Iglewicz & Hoaglin 1993), and median-rule (Carling 1998) on our data. The modified Z-score method is similar to $n \times \sigma$ -clipping, but instead of mean and SD, the median and MAD_e⁵ are used. Median-rule is a modification of Tukey’s (boxplot) method (Tukey 1977) and defines outliers as points that lies further than $\text{median} \pm k \times \text{IQR}$, where IQR is the interquartile range. We varied the k to {2, 2.5, 3} for the σ -clipping and median-rule, and $k = \{2.5, 3, 3.5\}$ for the modified Z-score. The selected values of k are within the intervals suggested in the above cited references.

A potential difficulty that one faces when trying to remove outliers is the so-called masking and swamping effects - removal of one outlier changes the “status” of the other data points

⁵ MAD_e = 1.483×MAD, and is equal to SD for large normal data

³ Vienna Atomic Line Database

⁴ This line-list was subsequently analyzed in Adibekyan et al. (2015) to select a sub-list of lines suitable for abundance derivation for cool, evolved stars

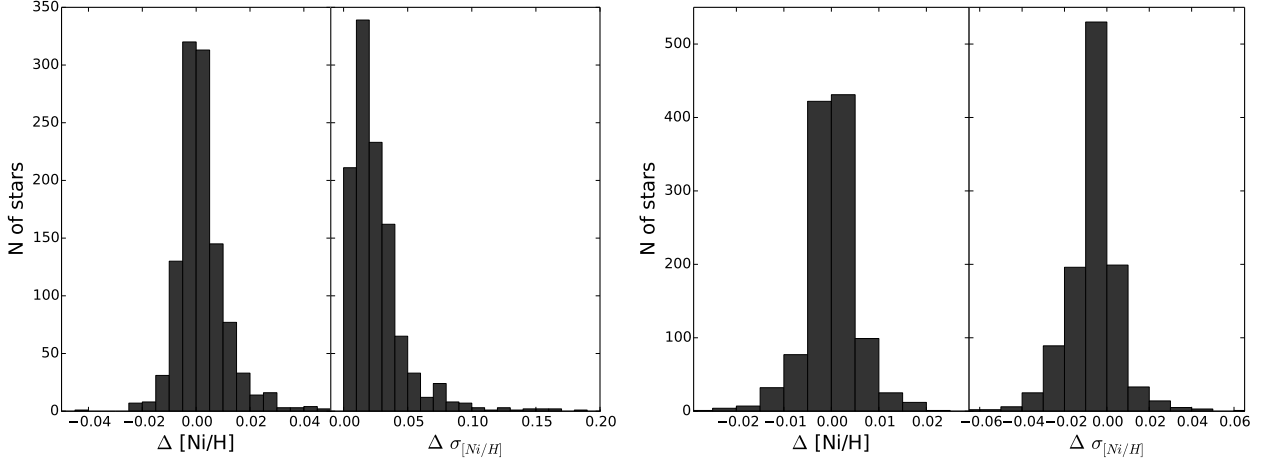


Figure A.1. Difference in $[\text{Ni}/\text{H}]$ and $\sigma_{[\text{Ni}/\text{H}]}$ when WM and AM without outlier removal methods are applied (left). The same as in the left panel, but the parameters are derived using WM and $\text{MAD}_e^{\text{iter}}$ (with the threshold of $\text{median} \pm 3\text{MAD}$) techniques.

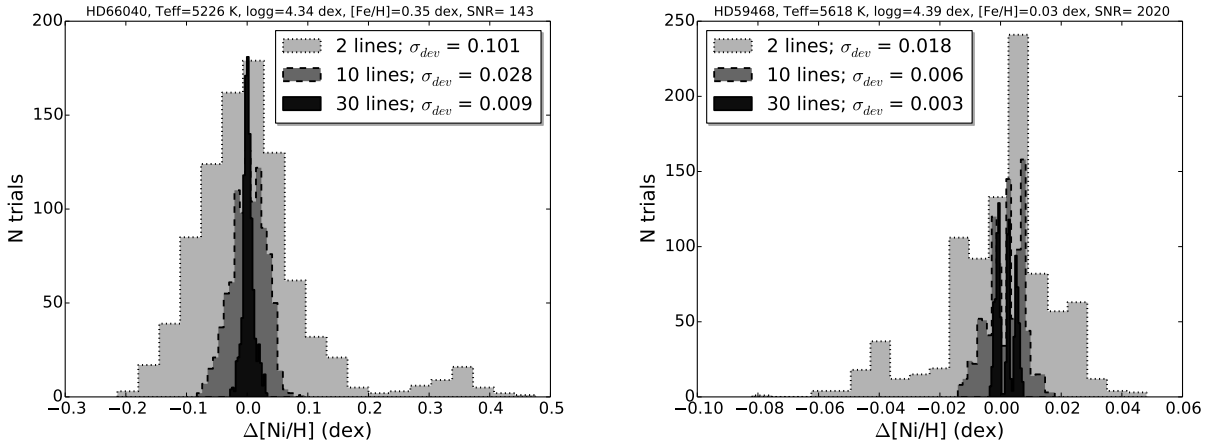


Figure A.2. The difference between original Ni abundance and Ni abundances derived with only 2, 10, and 30 Ni lines.

(Acuna & Rodriguez 2004). This means that it is advisable to remove one outlier at the time and apply the criteria recursively. However, it is not obvious when the outlier removal criteria should be stopped (the problem exists also when the outliers are removed at once). Two approaches were considered in our tests when modified Z-score method was used: i) remove all the outliers at once (we call it MAD_e technique in the remainder of the paper), and ii) remove one outlier at a time and then apply the criterion again iteratively (hereafter we call it $\text{MAD}_e^{\text{iter}}$ technique). For the second approach we allowed maximum number of 10 iterations, although in most of the cases, a lower number of iterations were needed (depending, of course, on the threshold accepted).

Outlier removal is not the only method used to characterize an underlying distribution in a dataset. An example is the weighted least-squares regression to minimize the effects of outlier data (Rousseeuw & Leroy 1987).

The last method that we use to calculate the final abundance and its line-to-line scatter is the WM and weighted SD. As a weight we used the (inverse) distance from the median value in terms of SD and then binned it. Using MAD and SD in the calculations of the weight on the average give very similar results, but if the values of more than the half of the points (lines) are the same (this can happen when the number of lines is small), then MAD is by definition zero, and cannot be used to calculate

the weight. Since the distance of the median point from the median is zero, the weight of that line would be infinite. To avoid giving a very high weight to the points that are initially close to the median (the final value would by construction be very close to the median), we decided to bin the distances with an interval of 0.5SD . E.g., a $0.5 \times \text{SD}$ weight was given to the lines that are at the distance from 0 to 0.5SD from the median. Similarly, a $1 \times \text{SD}$ weight was given to the lines lying at the distances of 0.5 to $1 \times \text{SD}$, and so on.

The results of our tests are summarized in the Table A.1. The test showed that all the outlier removal methods give a mean, final abundance similar to the one of the WM. Since the number of lines is relatively large, the impact of possible outliers is small, and all the values were also similar to the abundance calculated by the AM of all the points. However, we note that when the lowest thresholds were set to remove outliers, some stars due to the large number of removed “outliers”, showed deviations in the final abundance from the mean abundance derived from different methods. Another important point to stress is that when outlier removal methods were applied with low thresholds, the line-to-line scatter (which is usually used as an error estimate of the final abundance) was usually small, as expected.

From these tests (and further tests presented next in this work), we concluded that the best way to calculate the final abundance and its error is to use the WM. In this case, the weight of

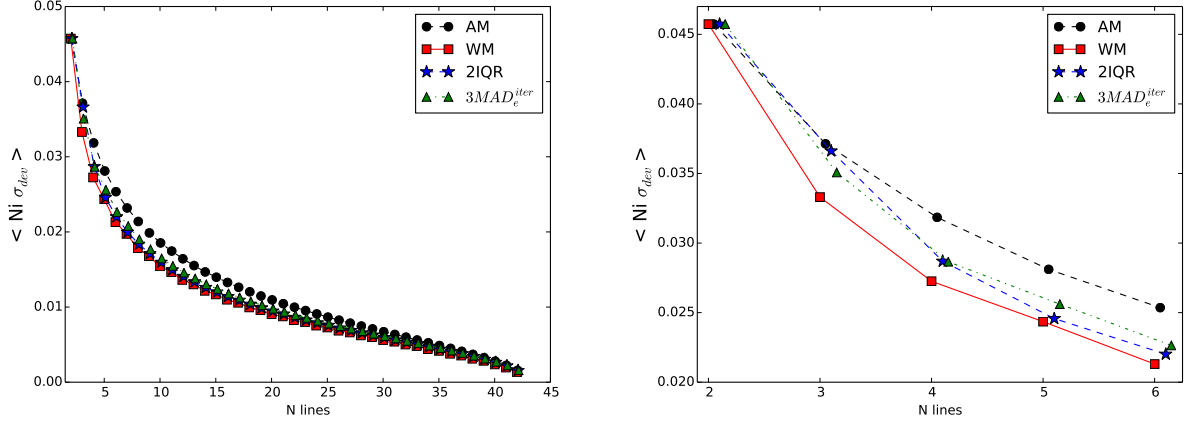


Figure A.3. Average deviation from the original Ni abundance for 1111 stars versus number of lines that were used for the abundance derivations. The *right* panel is the zoom of the left plot, only limited to six lines. Different techniques that were used in the calculations are mentioned in the plots.

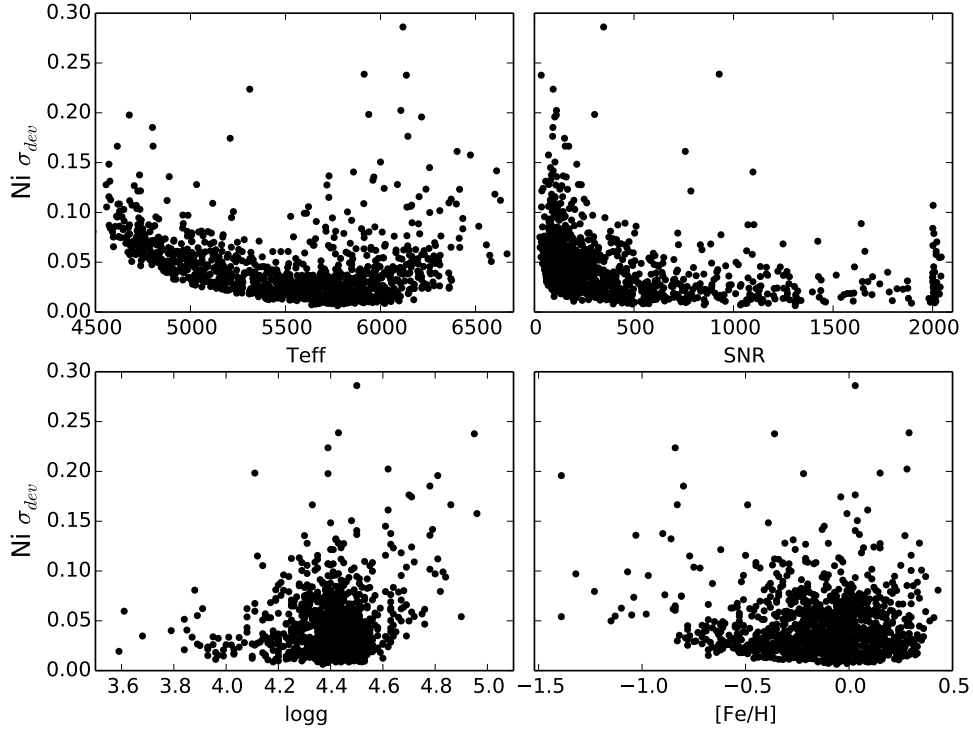


Figure A.4. Dependence of the average deviation from the original Ni abundance for 1111 stars versus stellar parameters and SNR. The abundance deviation represents the difference between original Ni abundance and Ni abundance derived only with 2 lines.

real outliers (extremes) is small, and the final abundance is not affected. With this approach, we also do not reduce the scatter by artificially removing points from the distribution. In Fig. A.1, we plot the distribution of the Ni abundance and its error (line-to-line dispersion) differences when WM and AM method is applied (left plot), and when WM and MAD_e^{iter} (median \pm 3MAD) criteria is applied (right plot). From the plot and table it is very clear that when the number of lines is large, different outlier removal (or not) methods provide very similar results for Ni abundances, however the error associated to these values depends on the method. In particular, Fig. A.1 shows (left plot) that line-to-line scatter of $[Ni/H]$ is always larger when the Ni abundance is calculated by the AM than when the WM method is used (the difference in $\sigma_{[Ni/H]}$ is always positive). The right panel of the

same figure, shows that the difference in $\sigma_{[Ni/H]}$ when Ni abundance is calculated by WM and MAD_e^{iter} , is usually small and can be both positive and negative.

A word of caution should be added at this point. In the methods that we tested to remove “outliers” and in the WM technique we assume that the distribution of the abundances (or the distribution of the errors on abundances) is symmetric⁶. However, as it was shown in Bertran de Lis et al. (2015) for very weak lines with an assumption of LTE (local thermodynamic equilibrium) the distribution of uncertainties of abundances is asymmetric.

⁶ Note that for the WM method there is no assumption on the normality of the distribution of the errors of abundances, while some outlier removal methods based on this assumption.

The authors also showed that this effect depends on the SNR and is negligible for lines with EW greater than $8\text{m}\text{\AA}$ regardless of SNR. However, since in all the methods are based on the same hypothesis, the WM technique remains favorable for us.

A.2. Abundance precision dependence on the number of lines

To evaluate the impact of the number of lines (that one uses for abundance derivations) on the abundances, we did the following simple tests. For each star in the sample, we randomly drew N Ni lines ($N = 2, 3, \dots, 42$) and calculated the Ni abundance. We used the above mentioned WM technique for the calculation of the abundances. Then we compared the resulting abundances with the supposed Ni abundance value (derived by using all the 43 lines available and the WM technique). If the number of possible combinations is less than 1000, we considered at all the possible combinations of lines, otherwise we drew $N=1000$ random, but different combinations of lines⁷.

In Fig. A.2, we plot an example (for two stars) of the distribution of the differences in Ni abundances ($\Delta[\text{Ni}/\text{H}]$) when three different number of Ni lines (2, 10, and 30 lines) and all the available lines are used. The stars have different stellar parameters and different SNR in the spectra. The plot shows that when the number of lines is increased the abundance difference gets smaller. It also shows that while most of the cases/trials the $\Delta[\text{Ni}/\text{H}]$ is close to zero, it is possible to obtain very large differences when only two lines are used (even for very high SNR data).

We did the aforementioned computations for all the 1111 stars and for each number of lines we calculated the standard deviation of $\Delta[\text{Ni}/\text{H}]$ distribution - σ_{dev} .

In Fig. A.3, we plot the dependence of the average of the σ_{dev} for all 1111 stars as a function of the number of lines. In the plot, we only limited ourselves with examples of four techniques with different thresholds in order not to overload the figure, while applying all the techniques and thresholds presented in Table A.1. Moreover, since in these tests the size of the sample (lines) varies, we decided to test also lower outlier removal thresholds: $k = 1.5$ for σ -clipping and median-rule methods, and $k=2$ for modified Z-score methods).

Fig. A.3 shows the range of possible deviations (1σ deviation if the distribution was a Gaussian) from the original value for a given random star when a randomly draw N lines are used. It clearly shows that the deviation decreases very steeply with the number of lines and becomes smaller than 0.01 dex when more than 15 lines is used.

On the right panel of Fig. A.3, we show that, for a number of lines less than or equal to six, there is a subtle difference between different outlier removal techniques. It clearly shows that the smallest average deviation is obtained when the WM is used. We note, that other tests with different thresholds show similar results. The low thresholds for outlier removal techniques give results closer to that obtained by using WM for small number of lines. However, when low thresholds are considered for a large number of lines, due to high number of excluded lines, the final results deviate from the abundances obtained by using WM method. For the remainder of the paper we use abundances calculated by the WM method, if another method is not specified. Here we should stress again that we plot the possible deviations

of Ni abundances averaged for 1111 stars. While these average values are small, the deviations for individual stars can be very significant (as demonstrated in Fig. A.2).

It is natural to expect that the observed deviations should depend chiefly on the quality of the data (e.g. SNR) and also on the atmospheric parameters of the stars. This is because e.g. spectral lines in cooler stars spectra are usually more blended, and also because e.g. different lines form at different layers of the atmospheres and have different sensitivities to the non-LTE effects. In Fig. A.4, we plot for the case in which only two lines were used the dependence of the average σ_{dev} on the stellar atmospheric parameters and on the SNR. The plot shows that there is only a strong and clear dependence on T_{eff} . This result is expected since at low temperatures the spectra of cool stars are crowded and line blending plays a stronger role. Lowest metallicity stars and stars with the lowest SNR also show somewhat larger deviations. It is interesting to note that even if the SNR is very high, depending on stellar parameters, it is possible to obtain a Ni abundance up to 0.1 dex different from the original abundance when only two Ni lines are used.

Appendix B: [X/Fe] star-to-star scatter: dependence on the number of lines

⁷ We note that 1000 is a sufficiently high number of combinations and our tests showed that increasing this number by a factor of 100 has negligible impact on the results.

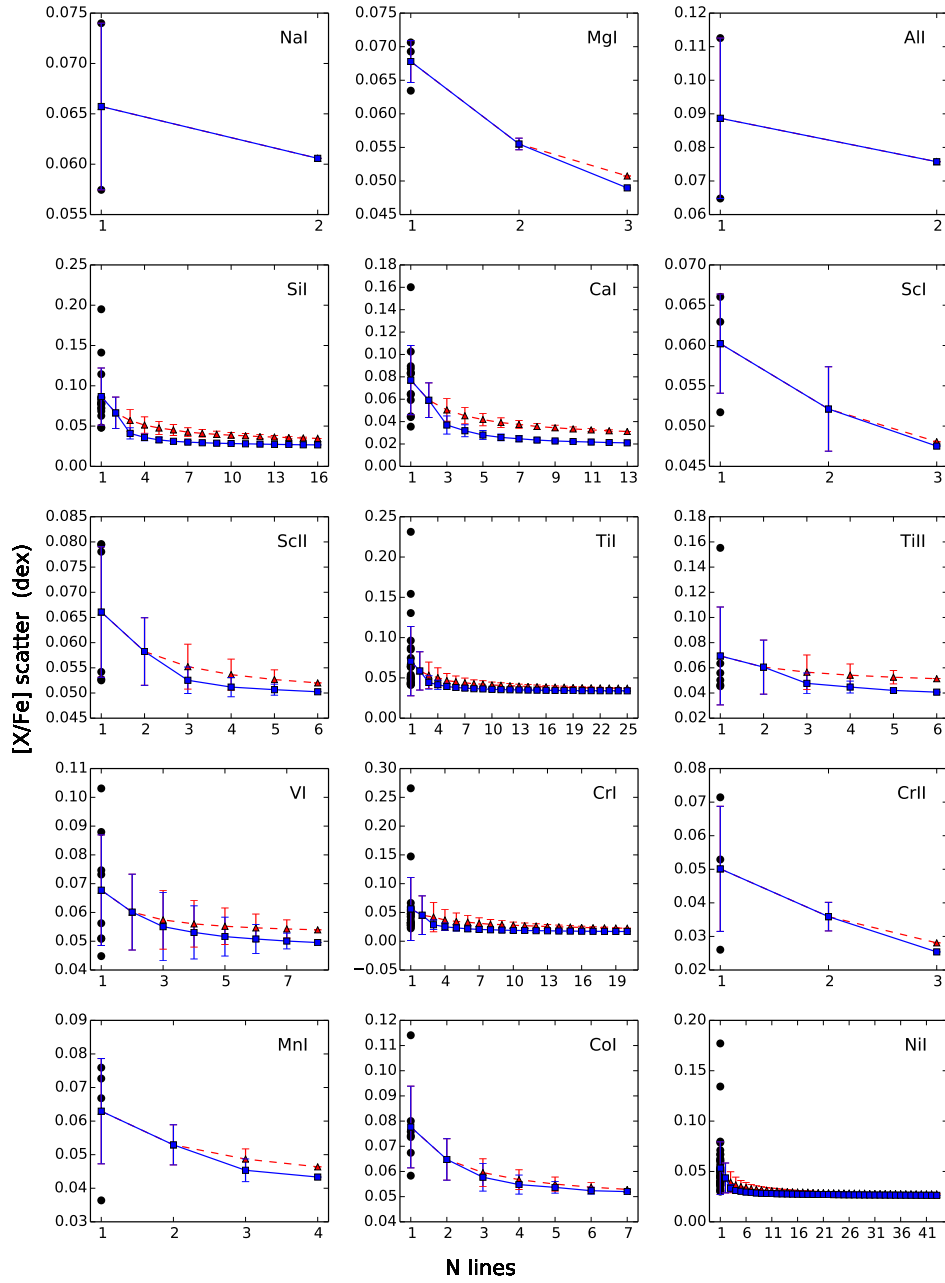


Figure B.1. Dependence of [X/Fe] star-to-star scatter for solar-analogs with $[Fe/H] = 0.0 \pm 0.10$ dex on the number of lines. Red triangles show the scatter when the individual abundances are calculated as an AM and the blue squares indicate the scatter in [X/Fe] when the WM method was used for the abundance derivation. The black dots show the [X/Fe] scatter for each individual line that was used to derive [X/H]. The error bars indicate the dispersion of possible combinations of the lines.